

- $^{13}\text{C}^{12}\text{C}_{60}\text{H}_2$ to be 843.0190 and found for both the 1,9 and 7,6 isomers to be 843.0192. Mass peaks were broadened by the isotope mixture. Unlike C_{60}H_2 , signals for the parent fullerene ions were not observed by FAB MS.
- The chemical shifts of the C_{70}H_2 isomers are ~ 2 ppm upfield from that of C_{60}H_2 in the same solvent, 8 5.93 ppm. This result may indicate that C_{70}H_2 is less acidic than C_{60}H_2 , the $\text{p}K_a$ of which is 4.8 ± 0.3 . D. H. Evans, paper presented at the Electrochemical Society Meeting, New Orleans, LA, 13 October 1993.
 - MNDO/PM3 heats of formation, relative to that of 7,8- C_{70}H_2 , for the 21,22 and 23,24 isomers are 7.08 and 48.45 kcal/mol [corresponding data from (3) for the 21,22 isomer is 6.80 kcal/mol]. Addition to the equatorial carbons is predicted to be extremely unfavorable. The calculated reaction of H_2 with C_{70} to give 23,24- C_{70}H_2 is endothermic by 11.20 kcal/mol.
 - For comparison, $^3J_{\text{HH}} = 14.3$ Hz for $\text{C}_{60}\text{H}_2\text{O}$ (dihydrate epoxide) and $^3J_{\text{HH}} = 14.1 \pm 0.5$ Hz for 1,2,3,4- C_{60}H_4 for the 6,6-ring fusion (only 9.8 ± 0.5 Hz for the 5,6 fusion). Other C_{60}H_4 isomers have coupling constants at 6,6-ring fusions of 15.5 to 15.8 Hz (C. C. Henderson, C. M. Rohlfing, R. A. Assink, P. A. Cahill, *Angew. Chem.*, in press).
 - The support is a Buckyclutcher I phase in which an unusually large amount of platinum remained from synthesis of the ligand.
 - Tighter error limits might result if (i) precise molar absorptivity data becomes available or if (ii) a catalyst that does not lead to hydrogen loss could be found. Such a catalyst would also be useful for studies of the isomerization of the multiple C_{60}H_4 isomers formed on reduction of C_{60} or C_{60}H_2 .

- Data on relative energies of C_{60}H_4 isomers derived from semiempirical calculations is therefore suspect [see, for example, N. Malsuzawa, T. Fukunaga, D. A. Dixon, *J. Phys. Chem.* **96**, 10747 (1992)]. We have repeated the C_{60}H_4 calculations at the HF/3-21G and HF/6-31G* levels and have found a markedly different energy ordering (C. C. Henderson, C. M. Rohlfing, R. A. Assink, P. A. Cahill, *Angew. Chem.*, in press).
- This work was supported under the Laboratory Directed Research and Development (LDRD) program at Sandia National Laboratories by the U.S. Department of Energy under contracts DE-AC04-76DP00789 and DE-AC04-94DP85000. We acknowledge R. A. Assink, D. R. Wheeler, C. Welch, R. Miilberg, and S. Mullen for helpful discussions.

5 November 1993; accepted 23 February 1994

A Mass Spectrometric Solution to the Address Problem of Combinatorial Libraries

Christopher L. Brummel, Irene N. W. Lee, Ying Zhou, Stephen J. Benkovic,* Nicholas Winograd*

The molecular weights of femtomole quantities of small peptides attached to polystyrene beads have been determined with imaging time-of-flight secondary ion mass spectrometry. The analysis is made possible by the selective clipping of the bond linking the peptide to a bead with trifluoroacetic acid vapor before the secondary ion mass spectrometry assay. The approach can be applied to large numbers of 30- to 60-micrometer polystyrene beads for the direct characterization of massive combinatorial libraries.

Combinatorial synthetic methods, which entail a series of chemical steps with multiple reagent choices for each step, can provide large repertoires of compounds with extensive molecular variation (1-8). Collections or libraries containing more than a million members have been created through synthesis on solid supports such as Merrifield beads (5, 7). The chemical identity of an oligonucleotide or peptide attached to a single bead can often be elucidated by microsequencing methods. For other families of compounds, the problem of identification has been solved by the attachment of tag molecules to the bead, thus encoding a history of the chemical operations. In the first of two recent examples, an oligonucleotide was cosynthesized alternating with each reagent addition. The resulting deoxynucleotide strand was then amplified and sequenced to determine the identity of the compound attached to the support bead (8). In the second example, a set of tagging molecules that encode a given reagent added in that step was attached to the supporting bead, and the process was repeated with additional sets of tagging molecules added during subsequent reagent addition steps. The collec-

tion of tags attached to a single supporting bead was liberated chemically and then identified by electron capture, capillary gas chromatography (9).

In this report, we propose a direct mass spectrometric assay that is generally applicable to the identification of the chemical nature of the compound on a single supporting bead in a large combinatorial library. This method does not depend on the synthesis of a tagging molecule or the attachment of sets of tagging molecules after each chemical separation. Although we illustrate the method for trimer peptides, the assay should ultimately prove useful in identifying a variety of pharmaceutically active agents.

We use imaging time-of-flight secondary ion mass spectrometry (TOF-SIMS) to identify the molecular weights of molecules bound to polystyrene bead surfaces (Fig. 1). This technology is potentially suited to such a problem (10, 11) because (i) molecular ions from a wide variety of precursors may be desorbed intact (12, 13); (ii) the parallel detection and high mass resolution associated with TOF detection provide a 10^4 - to 10^6 -fold improvement in sensitivity over scanning mass spectrometric methods (14); and (iii) the primary ion beam may be focused to a spot size of < 150 nm, so that the concentration of molecules can be mapped over small spatial domains (10, 11). Extreme sensitivity for an assay of the

kind proposed is obviously necessary. For example, a 40- μm sphere covered with one layer of Phe will only have 50 fmol of surface molecules available for sampling.

To test the feasibility of this approach, we examined the TOF-SIMS spectrum of a 40- μm polystyrene bead coated with about one molecular layer of Phe. This sample exhibits large peaks at mass-to-charge ratios (m/z) of 120 ($\text{M}-\text{CO}_2\text{H}^+$), 166 ($\text{M} + \text{H}^+$), 188 ($\text{M} + \text{Na}^+$), and 210 ($\text{M}-\text{H} + \text{Na}_2^+$) (Fig. 2A). Other peaks characteristic of bulk polystyrene (15) and Cu are also assignable. Phenylalanine was deposited on the bead by a simple physisorption procedure whereby the bead was immersed in a 10^{-4} M methanol solution of Phe, removed after several minutes, allowed to air-dry, and then placed on a Cu surface for analysis. For these measurements, the dose of incident 25-keV Ga^+ ions was controlled by limiting the sample exposure to 200,000 pulses (20 ns in duration each) of a 500-pA current. This exposure corresponds to 10^7

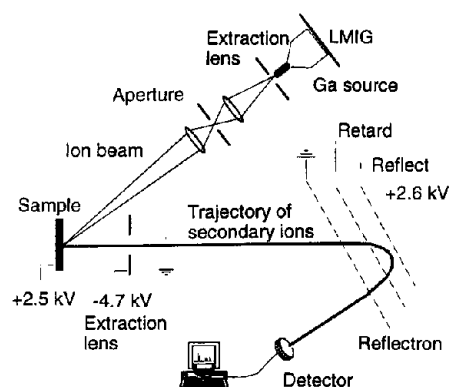


Fig. 1. Schematic diagram of the TOF-SIMS apparatus. Gallium ions from a liquid metal ion source (LMIG) are accelerated to 25 kV and are focused onto the sample with a spot size of ~ 150 nm. The beam is pulsed by rapid electrical deflection through an aperture typically for ~ 20 ns. Molecular ions sputtered from the sample are extracted through a field of 7.2 kV into a 2-m reflectron TOF analyzer. Ions are counted at a channel plate detector and processed by an online computer.

Department of Chemistry, Pennsylvania State University, 152 Davey Laboratory, University Park, PA 16802, USA.

*To whom correspondence should be addressed.

Ga^+ ions focused into a circular area $40 \mu\text{m}$ in diameter or $8 \times 10^{11} \text{Ga}^+$ ions per square centimeter. A 20-ns primary ion pulse yields a mass resolution of ~ 1500 at m/z 100. The low dose of primary ions ensures that sample damage does not alter the chemical nature of the target surface (16). Sensitivity varied depending on the molecular character of the sample being studied. For Phe adsorbed on a polystyrene bead, the detection limit is ~ 500 amol on a bead surface.

Our approach to the direct imaging of a combinatorial library of peptides adsorbed onto polystyrene beads is illustrated in Fig. 3A with the peptide Val-Tyr-Val prepared with the above procedure. For this assay, the pulsed Ga^+ ion beam is rastered across the $100\text{-}\mu\text{m}$ field, during which time a TOF-SIMS spectrum is recorded for each $\sim 1\text{-}\mu\text{m}^2$ pixel. An image is rendered by mapping of the intensity of $(M + H)$, $(M + \text{Na})^+$, and $(M - H + \text{Na}_2)^+$ ions at m/z 380, 402, and 424, respectively. For Val-Tyr-Val, the intensity is generally 0 to 4 counts per pixel. In spite of these relatively low count rates, a clear image of the coated bead is easily discernible. We estimate a detection limit of 2 fmol for Val-Tyr-Val.

There are several features of the data shown in Fig. 3A that need further elaboration. First, although the substrate is electrically conductive, the bead itself is an electrical insulator subject to charging. Normally, in static TOF-SIMS experiments, charging is not a significant problem because of the small number of incident ions needed to record a spectrum. For the imaging of small areas, however, ion current densities are much higher and some type of charge compensation is essential. In our experiments, the sample was flooded with 50 nA/cm^2 of 30-eV electrons for $50 \mu\text{s}$ between each Ga^+ ion pulse to eliminate charging artifacts (17, 18). A second issue involves the influence of the shape of the bead and the angle of incidence of the Ga^+ ion. In our configuration, the Ga^+ ion beam is incident at 45° from the surface normal (from the left in Fig. 3). The polystyrene sphere is $\sim 60 \mu\text{m}$ high and is placed in a 3-mm extraction gap with a field of 7200 V. Thus, in addition to problems dictated by the morphology of the bead, there is a 150-V field gradient across the bead. Both of these effects tend to produce higher signals near the leading edge of the bead. Finally, each of the assays reported here was completed in less than 4 min. The analysis time is determined by the flux of incident ions and the time required to reach the damage threshold. For small beads or higher current sources (or both), the analysis time could be reduced an order of magnitude.

Similar results to those shown in Fig. 3 have been obtained with Gly-Pro-Gly-Gly as well as a variety of other small peptides.

Bradykinin, with 11 amino acid residues, could be detected when adsorbed onto a polystyrene film (19), but we have yet to obtain a sufficiently large signal to generate an image from a $40\text{-}\mu\text{m}$ bead. Because combinatorial libraries of peptides on polystyrene beads generally consist of linear chains of three to six amino acids, the range imaged by TOF-SIMS appears to be sufficient to determine the parent molecular ion of the adsorbed peptides.

For peptides physisorbed onto the polystyrene beads, imaging TOF-SIMS provides a simple and direct assay of molecular weight. For the determination of a particular peptide address, however, it is necessary to desorb intact peptides directly that are covalently attached to the polystyrene surface. We find

that the formation of this covalent bond dramatically reduces the yield of molecular ions in the SIMS spectrum. This effect is shown in Fig. 2B for Phe covalently attached to a polystyrene bead where the yield of $(M + H)^+$ at m/z 166 is no longer visible, although strong fragment ions are found at m/z 120. In general, molecular ions for other peptides covalently bound to the bead were not observed and the spectra were found to consist mainly of intense fragment ions from protecting groups and of amino acid fragments. For example, with the pentapeptide Leu-Ser-Arg-Ile-Val, the molecular ion at $587 m/z$ was not observed nor were any of the cationized species, although several fragment ions typical of each of the monomer units (20) were easily found in the low mass range.

Fig. 2. Mass spectra of Phe attached to a polystyrene bead (A) by physisorption, (B) by covalent bonding, and (C) after vapor-phase clipping with trifluoroacetic acid. Peaks in the low mass region at m/z 23 (Na); 39 (K); and 63, 65 (Cu) are always observed as part of the background. In addition, a smaller contribution of polystyrene (PS)-derived peaks are also seen at m/z 91 (C_7H_7); and 103, 105, 115, 117, 127, 128, 129, 141, 152, 165, 178, 190, 193 (PS). The important Phe-derived features are indicated. Note the presence of $(M + \text{Na})^+$ and $(M + \text{Na}_2)^+$ features. These peaks may confuse molecular weight determinations, although characteristic mass differences are often obvious. The spectrum in C displays a prominent peak at m/z 147 due to a polydimethylsiloxane impurity that often finds its way to the surface of polystyrene.

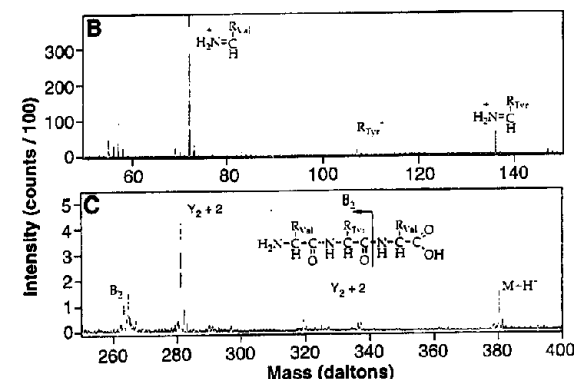
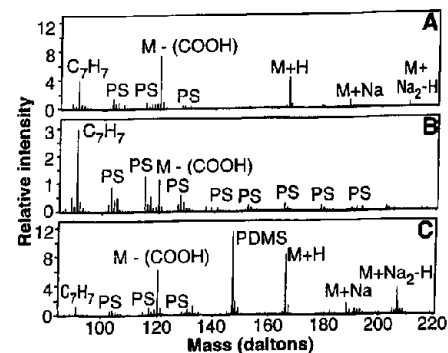


Fig. 3. (A) The TOF-SIMS image of a polystyrene bead covered with Val-Tyr-Val. The image was created by the monitoring of $(M + H)^+$, $(M + \text{Na})^+$, and $(M - H + \text{Na}_2)^+$ at m/z 380, 402, and 404, respectively. The field of view is $100 \mu\text{m}$. (B and C) The mass spectrum was collected from Val-Tyr-Val initially covalently attached to a single bead and subsequently clipped by the vapor-phase clipping procedure. The immonium ion for the individual amino acids is prominent in the low mass region at 73 and 136 amu for Val and Tyr, respectively. Tyr gives another fragment corresponding to the side chain at 107 amu. The high mass region shows $M + H$ at 380 and two fragments derived from two amino acid cleavages. The B_2 fragment is generated by a break in the peptide bond between the Tyr and the second Val and extends to the amino terminus, mass 263. The $Y_2 + 2$ fragment arises from the cleavage of the first peptide bond and extends to the carboxy terminus with the addition of two hydrogens, mass 281 (22).

To circumvent this difficulty, we have developed a protocol for clipping the covalent surface attachment while leaving the peptide resting in place on the bead. To begin, we selected a bead with an acid-sensitive linker as the substrate (21). Beads with covalently attached amino acids were then transferred to a Cu grid. The Cu grid is used as a support, and markings on the grid can be used to locate specific beads. The beads were then placed in a chamber saturated with trifluoroacetic acid (TFA) and methylene chloride (CH_2Cl_2) vapors from a TFA (15%) in CH_2Cl_2 solution. A 3-min exposure was sufficient to cleave the amino acid from the bead. The progress of the reaction was monitored by the observation of a color change from off-white to

purple on the beads themselves. Once the cleavage reaction was complete, the beads and Cu grid were inserted directly into the TOF-SIMS apparatus for analysis.

The mass spectra of the beads subjected to this vapor-phase clipping exhibited a strong signal for their corresponding parent ions. The SIMS spectrum of the clipped Phe is shown in Fig. 2C, while the corresponding image of m/z 166 is shown in Fig. 4A. The amino acid is confined to the bead, because its signal is not found from the surrounding Cu grid. However, the signals observed for Phe in Fig. 4A are more intense than the signals for Phe when it was simply physisorbed to a bead, perhaps because of the better uniformity of coverage resulting from the initial covalent bond formation. Thus, larger signals should appear from peptides clipped from the beads than from those prepared by other methods. The technique was further tested by the imaging of a mixture of Phe- and Leu-coated beads. The beads were placed on a Cu grid and cleaved with TFA as described above (Fig. 4B). Although the beads are very close to each other, there is no significant cross contamination.

The method was then extended to the tripeptide Val-Tyr-Val covalently attached through an acid-sensitive linker to the bead. The bead was subjected to clipping by the vapor-phase method and subjected to characterization by TOF-SIMS. The mass spectrum displayed in Fig. 3C shows ions at m/z 380 ($M + H$), 281, and 263. In the low mass range (Fig. 3B), intense peaks were found at m/z 72 (Val- CO_2H) and 136 (Tyr- CO_2H). The TOF-SIMS spectrum is sufficient to establish uniquely not only the composition but the Val-Tyr-Val sequence through the above fragmentation pattern. The use of fragment sequence ions to determine the structure of small peptides is well established (22).

This method will provide a determination of the mass of the parent ion and will identify directly those members of a library with a given molecular weight. The TOF-SIMS mass accuracy is now on the order of ± 0.01 atomic mass unit (amu) (10, 11). In a pentapeptide created from all 20 amino acids, there are 42,504 compositional peptides differing in their parent amino acids. Although many of these peptides have the same molecular weight [for example, Phe-Trp-Trp-Trp-Asn and Phe-Trp-Trp-Trp-His (molecular weight of 837.36)], they can be readily distinguished from one another by the presence of the monomer unit in the spectrum as noted above. Consequently, all compositional library members should be identified. The only naturally occurring amino acids that cannot be differentiated by mass are Leu and Ile. To distinguish between the two, a ^{15}N label can be incorporated into one.

In the case of permutational isomers (for the pentapeptide example there are 3.2 million members in this library), the fragment ions must be used to distinguish between members. A complete set of fragment ions is generally observed for peptides of fewer than 10 amino acids (22). Alternatively, a termination sequence strategy in which a small fraction of the growing peptide chain is deliberately capped chemically is included in the synthesis. Such termination sequences give rise to different molecular weights; the difference between the two such sequences is the last amino acid added (23, 24). Given the sensitivity of the TOF-SIMS procedure, this strategy may also be implemented.

There are many prospects for generalizing this chemistry. For example, our results show the importance of the surface chemical bond in controlling the detailed desorption event in many types of related SIMS experiments. These results suggest that alternative linker chemistry may enhance the molecular ion signal of covalently attached species. Further increases of sensitivity may also become feasible with special cationization schemes or by laser positionization of sputtered neutral molecules (25). It will be valuable to compare these results with ongoing molecular dynamics computer simulations of the ion bombardment event (26) to elucidate the energy transfer mechanisms that lead to molecular desorption and fragmentation. Finally, this methodology should not be limited to amino acids but should be applied, for example, to the addressing of libraries consisting of heterocycles such as benzodiazepines (2).

REFERENCES AND NOTES

1. M. J. Kerr, S. C. Banville, R. N. Zuckermann, *J. Am. Chem. Soc.* 115, 2529 (1993).
2. B. A. Bunin and J. A. Ellman, *ibid.* 114, 10997 (1992).
3. S. P. A. Fodor *et al.*, *Science* 251, 767 (1991).
4. G. Jung and A. G. Beck-Sickinger, *Angew. Chem. Int. Ed. Engl.* 31, 367 (1992).
5. K. S. Lam *et al.*, *Nature* 354, 82 (1991).
6. R. A. Houghton *et al.*, *ibid.*, p. 84.
7. B. G. Barany and R. B. Merrifield, in *The Peptides*, E. Gross and J. Meienhofer, Eds. (Academic Press, New York, 1980).
8. S. Brenner and R. A. Lerner, *Proc. Natl. Acad. Sci. U.S.A.* 89, 5381 (1992).
9. M. H. J. Ohmeyer *et al.*, *ibid.* 90, 10922 (1993).
10. N. Winograd, *Anal. Chem.* 65, 622A (1993).
11. A. Benninghoven, B. Hagenhoff, E. Niehuis, *ibid.*, p. 630A.
12. R. Beavis, W. Ens, K. G. Standing, J. B. Westmore, *Int. J. Mass Spectrom. Ion Phys.* 46, 471 (1983).
13. M. C. Davies, A. Brown, J. M. Newton, S. R. Chapman, *Surf. Interface Anal.* 11, 591 (1988).
14. B. T. Chait and K. G. Standing, *Int. J. Mass Spectrom. Ion Phys.* 40, 185 (1981).
15. G. J. Leggett, J. C. Vickerman, D. Briggs, M. J. Hearn, *J. Chem. Soc. Faraday Trans.* 88, 297 (1992).

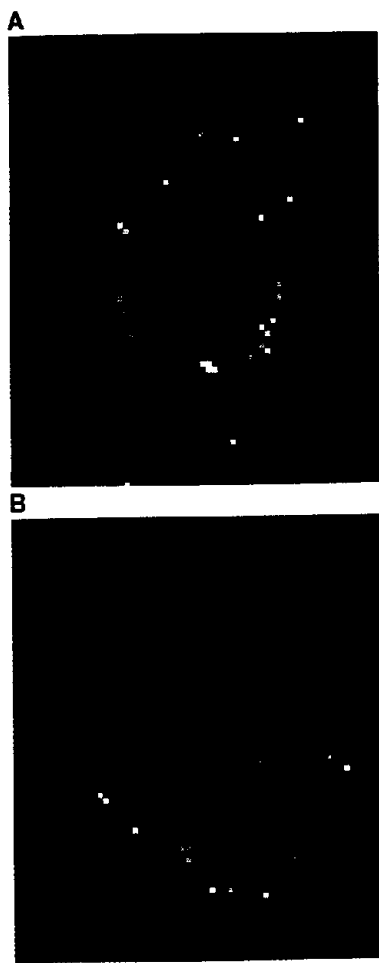


Fig. 4. The TOF-SIMS image of a mixture of beads with covalently bound amino acids placed on a Cu grid, after vapor-phase clipping. (A) The ($M + H$)⁺ ion intensity for Phe is shown in green, and the Cu^+ ion intensity is shown in red. (B) The ($M + H$)⁺ ion intensity for Phe is shown in green, while the ($M + H$)⁺ ion intensity for Leu is shown in red. The more brightly colored pixels contain more than one count. The primary ion beam is incident 45° from the surface normal (from the top). The field of view is 120 μm .

16. A. Benninghoven and W. Sichterman, *Anal. Chem.* **50**, 1180 (1978).
 17. J. A. Gardella and D. W. Hercules, *ibid.* **52**, 226 (1980).
 18. D. Briggs and A. G. Wooton, *Surf. Interface Anal.* **4**, 109 (1982).
 19. P. Steffens, E. Niehuis, T. Friese, D. Greifendorf, A. Benninghoven, *J. Vaccine Sci. Technol.* **A 3**, 1322 (1985).
 20. D. S. Mantus, B. D. Ratner, B. A. Carlson, J. E. Moulder, *Anal. Chem.* **65**, 1431 (1993).
 21. For this work, we have chosen a Sasrin bead

from Bachem Bioscience [M. Megler, R. Tanner, J. Gostelli, P. Grogg, *Tetrahedron Lett.* **29**, 4005 (1988); M. Megler, R. Nyfeler, R. Tanner, J. Gostelli, P. Grogg, *ibid.*, p. 4009].
 22. The B_2 and $Y_2 + 2$ cleavage mechanisms are discussed in K. Biemann and S. A. Martin, *Mass Spectrom. Rev.* **6**, 1 (1987).
 23. R. S. Youngquist, G. R. Fuentes, M. P. Lacey, T. Keough, *Rapid Commun. Mass Spectrom.* **8**, 77 (1994).
 24. B. T. Chait, R. Wang, R. C. Beavis, S. B. H. Kent, *Science* **262**, 89 (1993).

25. N. Winograd, Y. Zhou, M. Wood, S. Lakiszak, *Inst. Phys. Conf. Ser.* **128**, 259 (1992).
 26. R. Taylor and B. J. Garrison, *J. Am. Chem. Soc.*, in press.
 27. We thank M. Wood and J. Vickerman for helpful discussions. Supported by the National Institutes of Health, the National Science Foundation, the Department of Energy, the Office of Naval Research, and SmithKline Beecham.

23 November 1993; accepted 7 March 1994

Antiferromagnetic Ordering and Paramagnetic Behavior of Ferromagnetic Cu_6 and Cu_{18} Clusters in BaCuO_{2+x}

Z.-R. Wang, X.-L. Wang, J. A. Fernandez-Baca, D. C. Johnston, D. Vaknin*

Magnetization and neutron diffraction measurements on polycrystalline BaCuO_{2+x} revealed a combination of magnetic behaviors. The Cu_6 ring clusters and Cu_{18} sphere clusters in this compound had ferromagnetic ground states with large spins 3 and 9, respectively. The Cu_6 rings ordered antiferromagnetically below the Néel temperature $T_N = 15 \pm 0.5$ kelvin, whereas the Cu_{18} spheres remained paramagnetic down to 2 kelvin. The ordered moment below T_N was 0.89(5) Bohr magnetons per Cu in the Cu_6 rings, demonstrating that quantum fluctuation effects are small in these atomic clusters. The Cu_{18} clusters are predicted to exhibit ferromagnetic intercluster order below about 1 kelvin.

The strong antiferromagnetic (AF) coupling between the Cu spins in the CuO_2 planes of the undoped parent compounds of the high transition temperature cuprate superconductors (1) results from an indirect 180° bond angle $\text{Cu}^{2+}-\text{O}^{2-}-\text{Cu}^{2+}$ superexchange interaction ($J \sim 1000$ K). Aharony *et al.* (2) have argued that an intervening O^{1-} ion produced by a localized doped hole on the O^{2-} ion results instead in an indirect ferromagnetic (FM) interaction between the adjacent Cu spins, which in turn was predicted to strongly modify the magnetic properties of the parent cuprate. It is thus important to further clarify the conditions under which FM versus AF Cu-Cu interactions occur in copper oxides. An alternative cause of the FM interactions has been predicted to be a change in the Cu-O-Cu bond angle from 180° to 90° (3); however, the intermediate angle at which the crossover from AF to FM coupling occurs is unknown.

Here, we summarize a study of the magnetic properties of the compound BaCuO_{2+x} . Despite its simple chemical formula, this compound has a large body-centered-cubic (bcc) unit cell (space group $Im\bar{3}m$, $a = 18.25$ Å) with 90 formula units per unit cell (4, 5). The cell contains six lone CuO_4 units, eight

Cu_6O_{12} ring clusters, and two $\text{Cu}_{18}\text{O}_{24}$ sphere clusters formed from edge-shared CuO_4 units (Fig. 1). The Cu_6O_{12} ring clusters are formed by six edge-shared CuO_4 squares. The Cu-O-Cu bond angle in a six-membered and eight-membered ring is 75.5° and 81.6° , respectively. Magnetic susceptibility $[\chi(T)]$ measurements (5-7) of the compound showed Curie-Weiss-like behavior with a clear deviation from linearity below a temperature (T) of about 100 K. Electron spin resonance (ESR) measurements of the same compound (5, 8) indicated a phase transition at ~ 15 K. Preliminary neutron scattering measurements (9) on polycrystalline samples showed a phase transition at 13 K, consistent with the ESR studies. Unpolarized and polarized neutron diffraction measurements combined with magnetization measurements revealed that BaCuO_{2+x} exhibits a combination of magnetic behaviors. The Cu_6 and Cu_{18} clusters have FM ground states with large spins $S_r = 3$ and $S_s = 9$, respectively. The Cu_6 rings exhibit long range AF intercluster order below $T_N = 15$ K, with no apparent magnetic coupling to the lone Cu ions or the Cu_{18} clusters. In contrast, these latter two species remain paramagnetic down to 2 K and interact antiferromagnetically with an effective coupling strength $J = 1.1$ meV. Extrapolation of the magnetic susceptibility $\chi(T)$ data below 2 K predicts that the Cu_{18} clusters should exhibit FM intercluster order below ~ 1 K. Our results are relevant to many cuprate superconductors which show buckling of the CuO_2 planes and

significant deviations of the Cu-O-Cu bond angle from 180° , and to engineering new cuprates with novel properties.

A 1:1 molar mixture of BaCO_3 (99.99%) and CuO (99.99%) was thoroughly ground and heated to 800°C for 24 hours. The sample was then repeatedly reground and fired at 925°C for 24 hours. The sample was finally reheated to 900°C for 10 hours and cooled to room temperature (T) at a rate of 10°C per hour under He gas. Magnetization (M) data were obtained with a Quantum Design superconducting quantum interference device (SQUID) magnetometer.

The inverse of the molar magnetic susceptibility, $\chi = M/H$, for BaCuO_{2+x} is plotted versus T from 2 to 400 K (Fig. 2) for applied magnetic fields $H = 500$ G and $H = 10$ kG. The data in Fig. 2A above ~ 300 K approach the linear Curie-Weiss law $\chi^{-1} = (T - \theta)/C$. The molar Curie constant is $C = N_A g^2 S(S + 1) \mu_B^2 / 3k_B$, where N_A is Avogadro's number, g and $S = 1/2$ are, respectively, the gyromag-

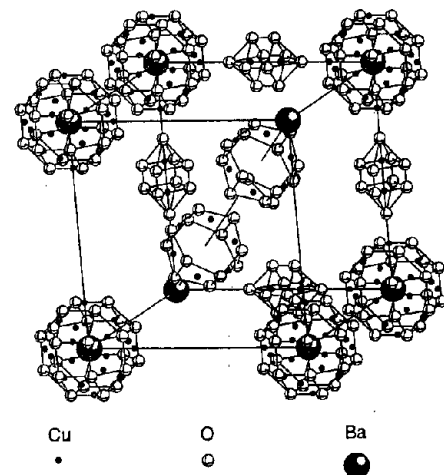


Fig. 1. Perspective representation of the two types of Cu/O clusters in the bcc unit cell of BaCuO_{2+x} . The $\text{Cu}_{18}\text{O}_{24}$ sphere-like clusters are located at the (000) and at the $(1/2, 1/2, 1/2)$ (not shown); the Cu_6O_{12} ring-like clusters are located at the $(1/4, 1/4, 1/4)$ and the remaining seven equivalent positions with their axis of highest symmetry along the corresponding body diagonal (only two rings are shown). The lone spins are located along principal directions adjacent to the spheres (partially occupied). Both clusters consist of closed one-dimensional strips of CuO_4 oxygen edge-sharing squares.

Z.-R. Wang, D. C. Johnston, D. Vaknin, Ames Laboratory and Department of Physics and Astronomy, Iowa State University, Ames, IA 50011, USA.
 X.-L. Wang and J. A. Fernandez-Baca, Oak Ridge National Laboratory, Oak Ridge, TN 37831, USA.

*To whom correspondence should be addressed.